BACHELOR THESIS

LUND UNIVERSITY

THEORETICAL PHYSICS

COMPUTATIONAL BIOLOGY

INCREASING MODEL ROBUSTNESS FOR STEM CELL REGULATION IN PLANT SHOOTS

Author:
Niklas KORSBO

Supervisor:
Prof. Henrik JÖNSSON

July 19, 2013

Contents

Abstract

The transcription factor WUSCHEL and the peptide CLAVATA3 have key roles to plat in the regulatory network effecting the differentiation of the stem cells at the shoot apical meristem of Arabidopsis.

The signal pathway of this network has been under investigation for several years and models utilizing the already identified parts of the network have been developed. Such models have however so far been unable to explain a buffering ability of WUSCHEL against certain perturbations made experimentally to the promoter strength of *CLAVATA3*.

For this thesis several alternative models have been proposed and investigated. All of them have a basis in a previously published model and adds or replaces different connections in order to be able to produce the experimentally observed dynamics.

These *in silico* experiments have yielded several new models that are able to explain the buffering capabilities of WUSCHEL. They also show that many types of self-activation of WUSCHEL can produce not only the WUSCHEL buffering dynamics, but also the dynamics of the additional six mutant experiments that were used as a basis for the previous model.

Chapter 1

Background

1.1 Meristem properties

The plant *Arabidopsis* has during the passed decades been used as a model plant to study the dynamics of different cell types in the plant shoot. There are different sites in the plant which contain stem cells, but the specific region of interest to this report is the shoot apical meristem (SAM).

The SAM is a region of a plant which can give rise to any above ground organ (Sablowski, 2007; Bleckmann and Simon, 2009). In order to maintain the pluripotency (the ability to give rise to many types of cells) of the stem cells while developing new organs the SAM contains several different types of cells which regulates the shape and the properties of the region (Schoof et al., 2000).

Different cell types exist in different zones of the SAM and contribute differently to the dynamics of the shoot. The stem cells are located at the very apex, in the so called Central Zone (CZ). These cells enables the plant to form new organs in the post-embryonic life of the plant. In creating a new organ a stem cell must differentiate and thereby loose its pluripotency. But as the plant can form new organs throughout its life the number of undifferentiated stem cells must be maintained. The stem cells in the CZ divide slowly and the cells that get pushed out of the CZ will instead enter the Peripheral Zone (PZ) in which they will start differentiating into the specific cell types required for the further development of the plant (Meyerowitz, 1997). The cells that remain in the CZ will however retain their pluripotency and allow for the process to repeat.

The cells of the CZ secrete a small extracellular protein called CLAVATA3 (CLV3) (Fletcher et al., 1999). This protein down-regulates the expression

of WUSCHEL (WUS) through a signal pathway that will be discussed below (Mayer et al., 1998; Schoof et al., 2000).

The transcription factor WUS is expressed in the Organizing Center (OC) from the gene *WUSCHEL*. The OC is the region right beneath the CZ which is believed to contain a large part of the regulatory function that determines the size of the CZ.

1.2 Regulatory dynamics

A primary feature of the studied network is the secretion of WUS which is required for the maintenance of stem cell identity of the cells in the CZ (Schoof et al., 2000).

In the network, which is represented in figure 1.1, CLV3 is transported from the CZ to the OC where it can bind to the receptor CLAVATA1 (CLV1) or to the receptor CORYNE (CRN), which are found at the cell membrane of the cells in the OC. The bound form of the receptors and the CLV3 then give rise to an intra-cellular signal which results in the repression of *WUS* transcription (Clark et al., 1997; Muller et al., 2008). Finally the feedback network is completed by the transportation of WUS from the OC to the CZ where it stimulates an increased expression of CLV3 (Yadav et al., 2011).

The major phenotypical effect of the network described comes from the regulation of WUS and CLV3. It has been shown that CLV3 functions as a promoter for differentiation of stem cells (Fletcher et al., 1999). Various CLAVATA mutants have been induced in Arabidopsis, and it is clear that over-expression of CLV3 will cause an increased differentiation of the stem cells and lead to a diminishing region of pluripotent cells and a decreased *WUS* activity (Yadav et al., 2010).

WUS however does the opposite, it promotes a maintained stem cell identity of the cells in the CZ. Over-expression of WUS lead to an expanding CZ, an increase in the number of stem cells and an increase in the number of organs formed from the SAM (Laux et al., 1996; Reddy and Meyerowitz, 2005).

1.3 Receptor mutants

In the investigation of the signaling pathway between CLV3 and WUS several receptor mutant experiments have been made. The following such mutants were used as a test set for the models:
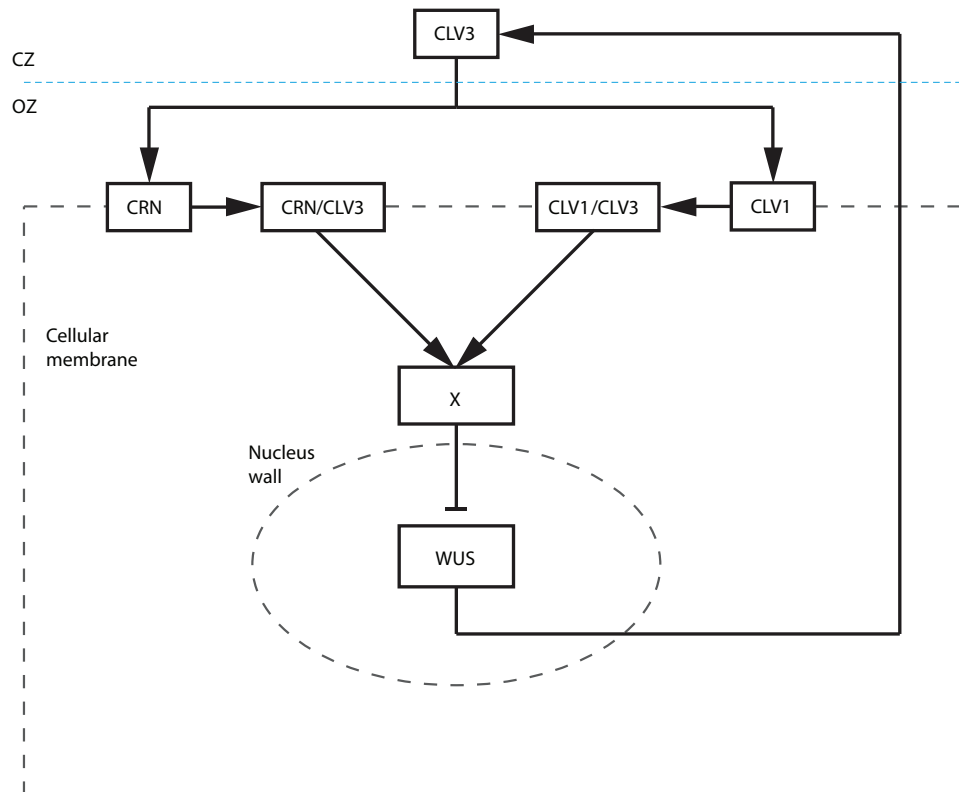
Figure 1.1: The regulatory network of the SAM as described in Sahlin et al. (2011). The gene *CLV3* is expressed in the CZ and the protein CLV3 is secreted. CLV3 reaches the OC and reacts with the receptors CLV1 and CRN located at a cell membrane. The receptor/CLV3 complexes gives rise to an unknown substance X which acts as a repressing transcription factor for *WUS*. The protein WUS is then transported to the CZ where it acts as an activating transcription factor for the production of CLV3.

clv1-1 a CLV1 Loss-of-function (LOF) mutant, rendering the CLV1 pathway less efficient.

clv1-11 a CLV1 null mutant, completely disabling the production of functional CLV1.

crn-1 a CRN LOF mutant, rendering the CRN pathway less efficient.

crn-1 clv2-1 a null mutant for the receptor CRN.

crn-1 clv1-11 a double mutant which causes LOF for the receptor CRN and disables the receptor CLV1.

crn-1 clv1-1 a double mutant which causes LOF for both the receptors CRN and CLV1.

The result of these mutants was measured by the phenotypical changes, changes to the actual appearance of the plant. This was especially quantified by the average number of carpels that grew from the SAM and these results are represented in table 1.1.

Mutant	Carpels
Wild type	2.0
crn-1	3.9
clv1-11 (null mutant)	3.9
crn-1 clv2-1 (null mutant)	3.8
clv1-1	4.2
crn-1 clv1-11	5.3
crn-1 clv1-1	4.5

Table 1.1: Mutants and their phenotypical effect. The first five items are the data optimized against in Sahlin et al. (2011) and the last two are the control mutants that were used to verify the parameter set.

1.4 Previous computational models

There are several computational models for the negative feedback network between CLV3 and WUS (Sahlin et al., 2011; Hohm et al., 2010; Fujita et al., 2011; Yadav et al., 2011, 2013). The backbone for all of the models that were attempted in this particular research project comes from the computational model that was published by Sahlin et al. (2011). It showed that a non-spatial model of differential equations (Methods) could successfully account

for the phenotypical difference between the wild-type (WT) and the six different mutant experiments listed in section 1.3.

The parameters of the model were optimized against the average carpel numbers of the receptor mutants represented in table 1.1 (Sahlin et al., 2011). By optimizing against data from the WT and four different mutants they were able to attain parameter sets such that the model could show the same equilibrium relations as experimentally seen for the mutants in question. Data from two additional mutant experiments were used as a filtering criteria for the attained parameter sets and in the end the model could fully account for the changes in phenotype for all the different mutants.

The major result of this model was to show that the conceptual setup seen in Figure (1.1), especially with the function of CRN, can account for the phenotypical effect of the clv1-1 (LOF) mutant being stronger than the effect of the clv1-11 (null) mutant. Normally a completely disabled mechanism should have a larger effect on a system then a mechanism with only reduced function. However if in this case CLV3 still binds to CLV1 but the signal from the complex is weak then it could have a greater effect then if it does not bind at all, leaving more CLV3 to bind to the still functioning CRN receptor instead.

1.5 Buffering dynamics

The Sahlin et al. (2011) model can produce the phenotypical effects of certain mutants of CLV1 and CRN in Arabidopsis. There is however a set of data that this model cannot account for.

It was shown by Müller et al. (2006) that the phenotype of Arabidopsis is remarkably robust to perturbations in the promoter strength of *CLV3*. They showed that *CLV3* promoter strengths ranging from 33% to 300% of WT does not effect the phenotype of the plant. At 16% of normal *CLV3* promoter strength the size of the SAM and the number of carpels increased, which is consistent with the previously mentioned effects of CLV3.

Since WUS is both necessary and sufficient for stem cell identity (Laux et al., 1996; Mayer et al., 1998) stability of the SAM size and carpel number indicate stability of WUS concentration. For this to be incorporated into a computational model the model must thus be able to account for a stable WUS concentration for perturbations ranging from 33% to 300% of WT CLV3 promoter strength. For stronger perturbations the model should behave as seen in other mutant experiments; over-differentiation of the stem cells for high concentrations of CLV3 and over-production of stem cells for low CLV3 and thus high WUS concentrations.

1.6 Modelling molecular dynamics

There are several ways to model molecular dynamics Among these is the non spatial mass action formalism which has been used throughout this research project. It is a deterministic approach which uses ordinary differential equations to attain the change rate of concentrations. The basic idea is that the rate of a reaction is proportional to the product of the concentrations of the reactants involved (Jönsson, 2012). A rate constant for the reaction will then represent the speed at which the reaction occurs, the time it takes for diffusion to make the molecules meet, the probability that a reaction occurs when the molecules meet, etc.. This simple way of modelling can be efficient at certain types of reactions given that the system reaction rate does not change with the effects of any diffusive behavior, that any of the other rate parameter representations are time dependent or that the number of molecules is so small that stochastic reaction fluctuations matter.

If for example the reaction

$$A + 2B \overset{k_+}{\underset{k_-}{\rightleftharpoons}} C$$
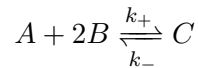
were to be modelled using mass action formalism it would yield:

$$\frac{d\,[C]}{dt} = -\frac{d\,[A]}{dt} = -\frac{1}{2}\frac{d\,[B]}{dt} = k_+\,[A]\,[B]^2 - k_-\,[C]$$

Transcription can be modelled by the use of Hill equations which is a version of Michaelis-Menten formalism.

The Hill equation for A acting as an activating transcription factor for B has the following appearance:

$$\frac{d[B]}{dt} = v_{\max}\frac{[A]^n}{K^n + [A]^n}$$

If A instead acts as a repressor the equation looks as follows:

$$\frac{d[B]}{dt} = v_{\max}\frac{K^n}{K^n + [A]^n}$$

The Hill formalism is a empirically, rather then mathematically, motivated alteration of the Michaelis-Menten which itself is derived from the mass action modelling of transcription or enzymatic reactions as

$$A + E \underset{k_2}{\overset{k_1}{\rightleftharpoons}} AE \xrightarrow{k_+} B + E$$
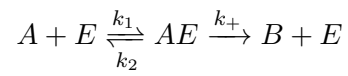
with the constraints that the amount of E is constant, k_+ is so much smaller than k_1 and k_2 that the left side of the reaction representation is in quasi-equilibrium. In the transcription case A would be a transcription factor, E the DNA and B the transcribed RNA.

Chapter 2

Results

A large amount of additional interactions was proposed and tested for the Sahlin et al. (2011) model. First the original model was analyzed by optimizing it using the buffering data. Then the focus was on finding a simple addition to the model which enabled it to produce a buffering capability of WUS. Rather than to presuppose the success of one or two model additions and testing them extensively a broad approach was taken, testing a multitude of possible propositions and discarding them if they did not show the desired dynamics.

2.1   A simple negative feedback between WUS and CLV3 cannot explain buffering

An analysis of the original model was made and it was found that the original model could not explain the Müller et al. (2006) buffering data, regardless of which parameter set was used. Despite the 19 parameters in the model there needs to be either non-linearities or competing, opposite, effects in the system of differential equations in order for it to be able to produce buffering. The Sahlin et al. (2011) model has no such competing effects, but there is one non-linear term in the effect of X on WUS. This non-linearity however cannot create the buffering capabilities seen in the CLV3 perturbation experiments.

This can be indicated analytically and becomes clear when the model is scaled down to the only dynamics that possibly could provide the WUS buffering capabilities. Removing as many of the linear steps as possible yet retaining a functional and representative network yields the following system of differential equations:

$$\begin{cases} \frac{d[\text{x}]}{dt} & \propto \quad a[\text{WUS}] - b[\text{x}] \\ \frac{d[\text{WUS}]}{dt} & \propto \quad \frac{c}{c+X} - [\text{WUS}] \end{cases} \tag{2.1}$$

where a is the constant that is changed by the perturbation experiment and x represents the total CLV3 signalling. WUS concentration at equilibrium will then have the following dynamics

$$[\text{WUS}](a) \propto \frac{1}{2a} + \sqrt{1 + \frac{1}{4a^2}} \tag{2.2}$$

which cannot explain the WUS plateau at any range of a

An optimization of the model against the *CLV3* promoter perturbation data was made to further indicate that it could not produce the WUS buffering behavior and to provide a reference for the other attempts to be compared with. None of the parameter sets attained from the optimization could produce the equilibrium relations sought (Figure 2.1). So in order for the model to be able to explain both the data used by Sahlin et al. (2011) and the perturbative data shown in Müller et al. (2006) reactions must be changed or added.
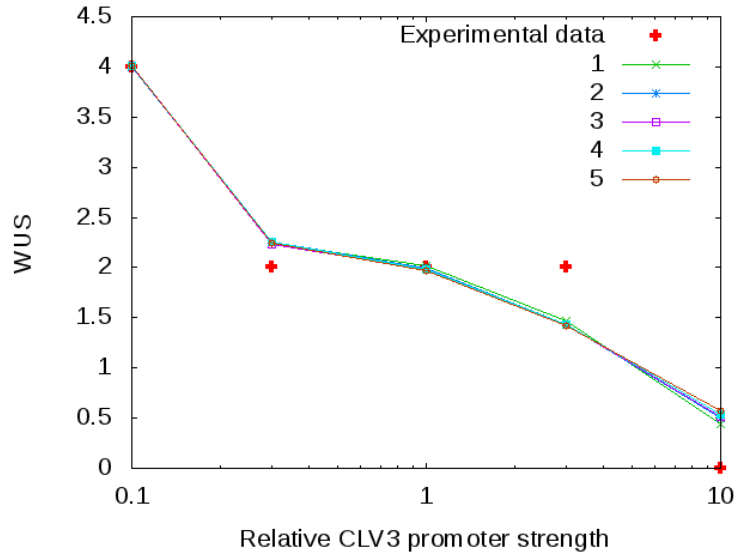

Figure 2.1: The results of the best five parameter sets out of 25 optimizations for the Sahlin et al. (2011) model in trying to reproduce the results shown in the CLV3 perturbation experiments. The model does not fully produce the required buffering of WUS against perturbations in CLV3 even when specifically and exclusively optimized against this.
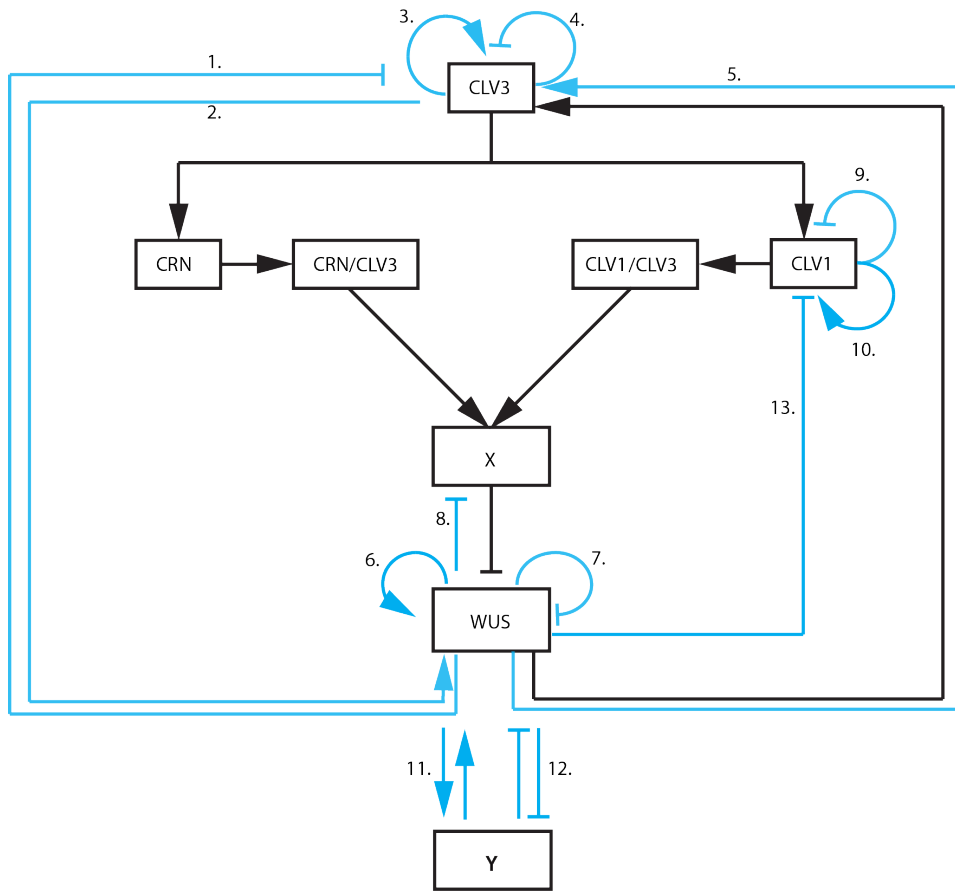
Figure 2.2: An overview of all the additional dynamics tested together with labeling for easier discussion of the different model attempts.

2.2 Self-activation of WUS produced all-over excellent results

A set of candidates for additional interactions were modelled and tested (Figure 2.2). 25 parameter optimizations were made against the WUS buffering, as seen in experiments. The approach gave distinct differences on the ability to account for the buffering for different model versions (Table 2.1). The best energy value attained was used as a criteria for further investigation. These models were then optimized against not only the CLV3 perturbation experiments, but also against all the data that were used to create and verify the Sahlin et al. (2011) model.

Path added	Brief description	Lowest energy value
13	Repression of CLV1 by WUS	6.9e-05
6	WUS self-activation	8.5e-05
8	Repression of X by WUS	0.00036
12	Indirect WUS activation through Y repression	0.00042
11	Indirect WUS activation through Y activation	0.00043
1	Hill repression and linear activation of CLV3 by WUS	0.0031
5	Hill activation replacing linear activation of CLV3 by WUS	0.0068
10	CLV1 self-activation	0.020
7	WUS self-repression	0.037
4	CLV3 self-repression	0.045
9	CLV1 self-repression	0.046
3	CLV3 self-activation	0.047
None	Unaltered model	0.054
2	Activation of WUS by CLV3	0.063
1	Hill repression replacing the linear activation of CLV3 by WUS	0.11

Table 2.1: 25 optimizations were made against only the WUS buffering for each of the proposed models. The best energy values attained for each model is listed here and only the six best performing models were tested further.
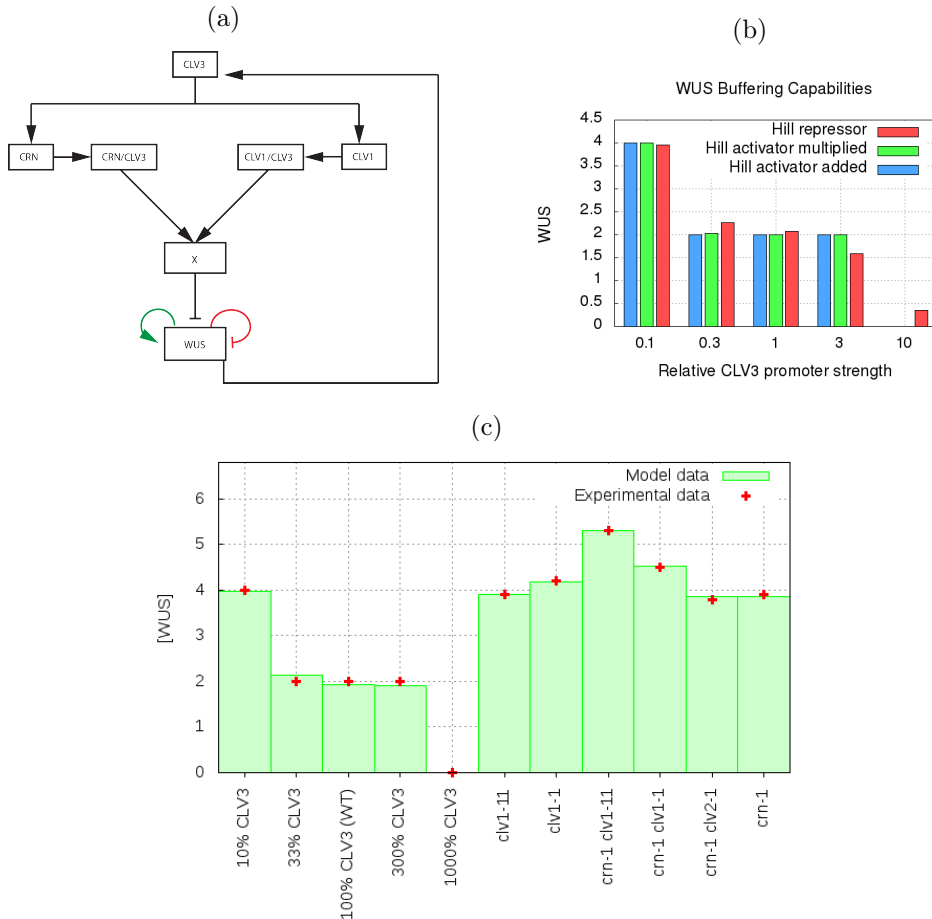
Figure 2.3: Direct self interaction of WUS was initially tried in three three different ways, two different logics for activation and one for repression (a). The models were optimized 25 times against the WUS buffering towards *CLV3* promoter perturbation and the best resulting dynamics for each model is shown in b) where both of the activator logics show an ability to perfectly produce the required buffering whereas repression does not. In c) direct Hill-type self-activation of WUS were examined and proved very effective at producing not only the dynamics seen in the CLV3 promoter mutants but also the dynamics of the receptor mutants, using the same parameter set.

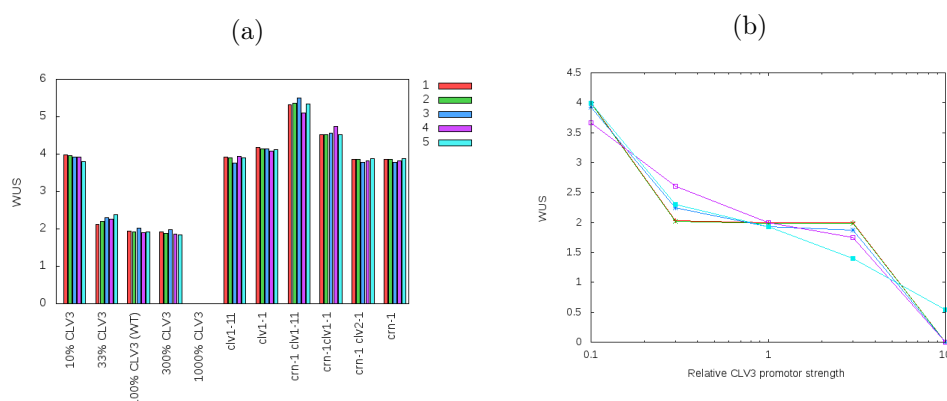(a)   (b)

Figure 2.4: a) show the five best buffering behaviours from the 25 optimizations initially done to the multiplied version of WUS self activation. Notice that despite 25 optimizations only three parameter sets allowed the model to show promising buffering capabilities. b) show the dynamics of the best 5 over-all fits to all the available mutant data from 85 optimizations. The behaviour of the model do not differ greatly with these parameter sets, but it is still quite noticeable. The parameter values used in b) are listed in table 4.1 of the appendix.

Despite a relatively large number of models that seem apt at producing a buffering ability of WUS only three mechanisms proved able to represent the full dynamics that is required of a successful model. These were the direct self-activation of WUS, the repression of X by WUS and WUS activating the WUS activator Y (models 6, 8 and 11). Interestingly, all of these successful attempts is some form of WUS self-activation.

Direct self-activation of WUS was tried using two different logics for modelling: adding or multiplying a hill activator to the hill type repression that X already asserts on WUS (Methods). Both of these alterations to the original model were able to produce the desired buffering capability of WUS (Figure 2.3). Neither of these models are likely to accurately depict reality. This as both of the models would ensure WUS production as long as any WUS exists, regardless of the rest of the system. Experiments have shown that an ectopic (driven by another promoter) expression of *WUS* in Arabidposis does not start up the normal *WUS* expression and thus direct self-activation of WUS is unlikely (Yadav et al., 2010). The results are however still informative as they give strong indications that *indirect* self-activation of WUS would work.

Simulations were performed using different parameter sets and the dynamical difference these produce was examined. In figure 2.4b the five best parameter sets from the optimizations against the WUS buffering are represented. It
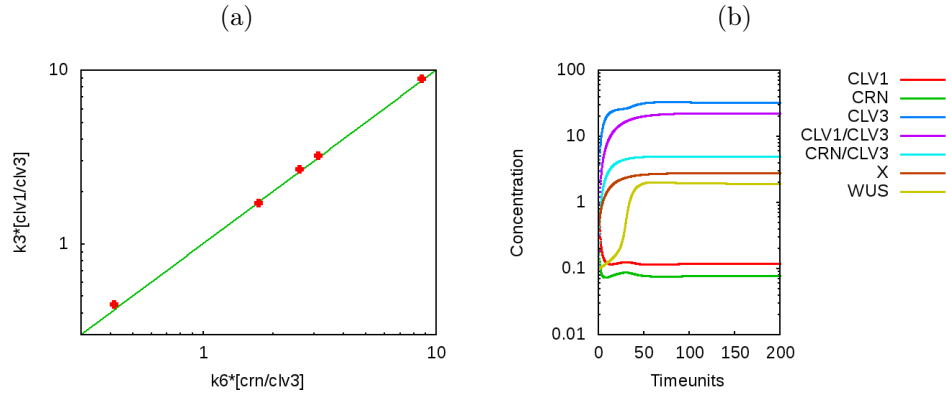
Figure 2.5: Behavioural analysis of the WUS self-activation model using successful parameter sets. a) show the relative strength of the CLV1 to CRN pathway for simulations using the five all-over best parameter sets (represented in table 4.1 and used in subfigure 2.4a). The closer a point is to the line y=x the smaller the difference in strength of the pathways. The simulation of a WT plant was used to attain this data and all of it shows that the pathways are equally strong. This agrees well with a similar analysis done by Sahlin et al. (2011) for their model. b) show the development of a system where all the concentrations were initiated with the value 0.1. The WT WUS self-activation model were used along with the best parameter set obtained for this model (parameter set 1 in table 4.1 of the appendix).

shows that there are parameter sets even amongst the top five that was unable to produce buffering, despite the proven success of this model. The relative strength of the network pathways CLV1 and CRN was examined by performing simulations of a WT representative model with WUS self-activation, multiplying the constant controlling the effect of the receptor/CLV3 bound state to X with the concentration of the bound state and comparing these (Figure 2.5a). This examination showed that the strength of the two pathways are almost identical for the five different parameter sets used (for parameter values, see Appendix). The best parameter set was also used to produce a graph of the dynamics of the different concentrations during equilibration. Here the sigmoidal curvature of the WUS concentration due to the Hill equation can clearly be seen (Figure 2.5b).

Direct self-repression of WUS was, as comparison, shown to be able to produce only a weak buffering tendency of the concentration of WUS for different CLV3 expression levels (Figure 2.3b). The produced result fit relatively poorly with the experimental data and after this assessment the model attempt was not pursued further.

2.3 Indirect WUS self-activation

After seeing the success of the direct WUS self-activation 5 different indirect self-activations were attempted (path 1, 8, 11, 12 and 13 in Figure 2.2). These are:

Model 1, in which a hill type repression of CLV3 by WUS was added, managed to produce buffering dynamics for WUS when optimized solely against this (see Figure 2.6b). However, no parameter set out of 50 optimizations were able to account for all the available experimental data at the same time (subfigure 2.6c).
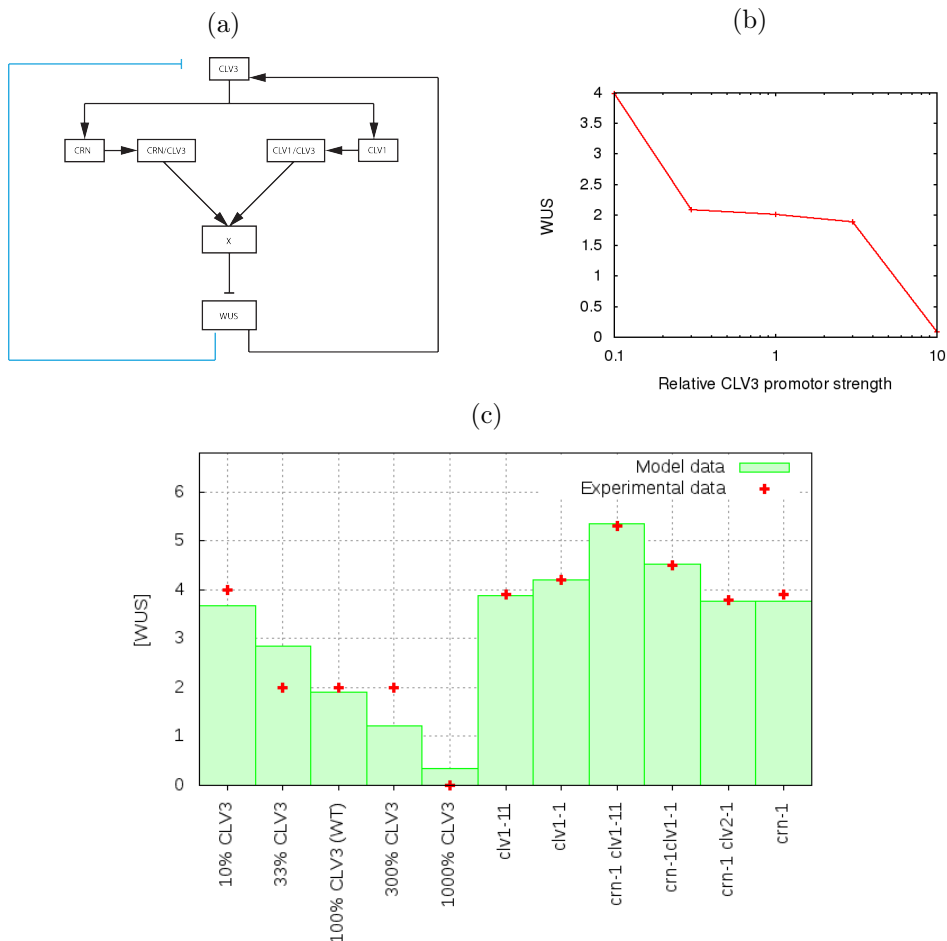
Figure 2.6: Model 1, in which linear activation and hill-type repression of CLV3 by WUS (a) resulted in WUS buffering for the initial 25 optimizations against the Müller et al. (2006) data (b). But when the model was optimized against all of the mutant data at the same time the required buffering dynamics was not seen (c).

Model 8, where WUS leads back to the intra-cellular CLV3 pathway, was apt at creating the buffering expected from WUS. It was modelled by removing the constant base-production of X and replacing it with a hill-type equation using WUS as a repressor. The best results from this attempt show that this model is capable of not only explaining a buffering of WUS but it is also able to explain the other mutant experiments using a single parameter set (Figure 2.7).

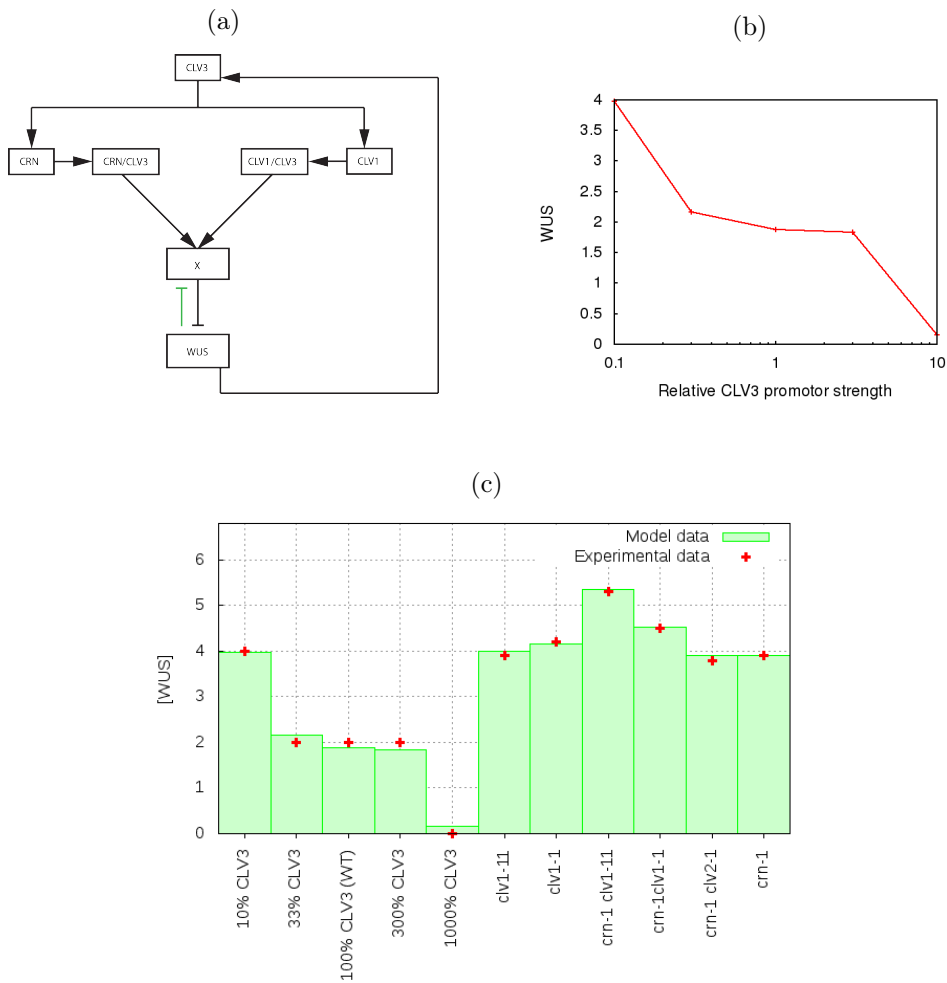Figure 2.7: Model 8, where WUS acts as a repressor on X (a) produced good results. b) show a good buffering capacity of WUS and c) show that this buffering and all the receptor mutant dynamics can be achieved by the model. This was not given, but it was not surprising seeing as this is an indirect self-activation of WUS with few intermediate steps, and direct WUS self-activation has proved to work.

Model 11 was built around an added compound Y that interacts with WUS. It was built to represent an unknown and very simplistic external network controlling the expression of WUS but could also conceivably represent interaction with ARR proteins as described by Zhao et al. (2010). Path 11 was modelled using Y which had a base production and degradation in combination with a Hill function that used WUS as an activator. Y in turn was the activator for a Hill function *multiplied* to the pre-existing Hill function that represents the WUS repression by X (Methods).
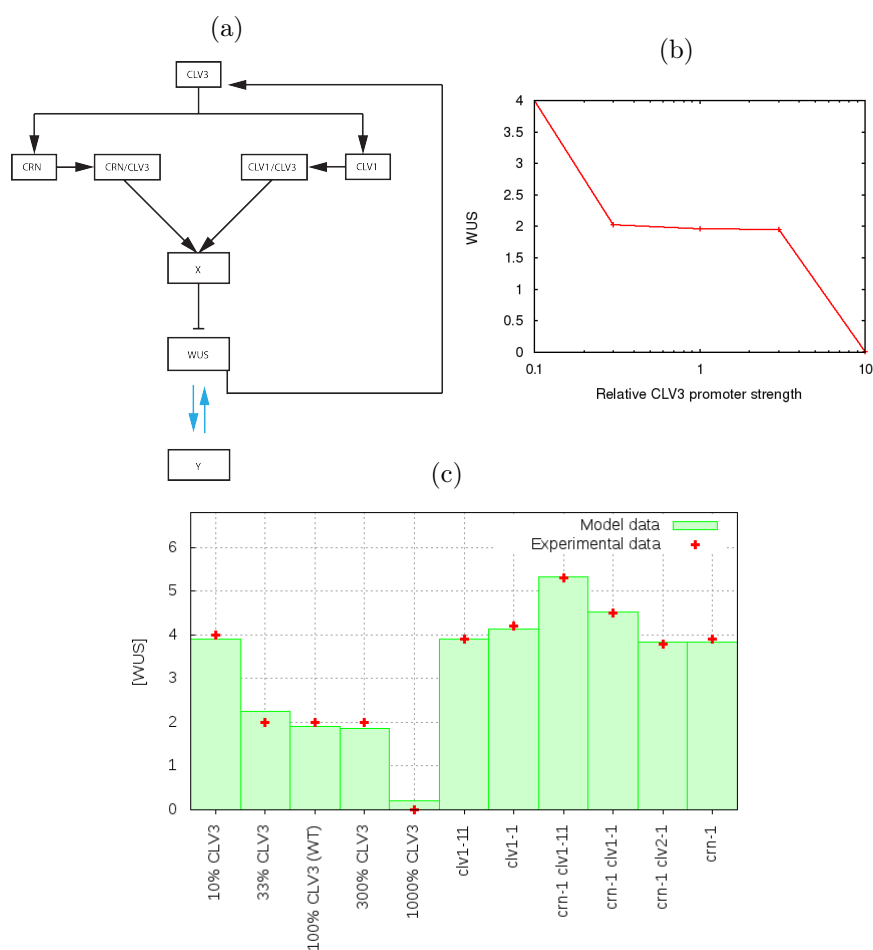
Figure 2.8: Model 11, in which WUS activation of an external activator Y (a) is able to produce almost perfect WUS buffering (b) and manages to produce good over-all dynamics when optimized and tested for all the mutants (c).

Path 12 was modelled in a similar way, but with hill repressors instead of activators. Somewhat surprisingly model 11 produced all-over good results, while model 12 did not manage to produce the combined WUS buffering with receptor mutant dynamics (Figures 2.8 and 2.9).

Figure 2.9: Model 12, in which WUS repression of an external repressor Y (a) proved effective at producing buffering dynamics for WUS (b) but did not, using any of the attained parameter sets, manage to produce all the required dynamics from the mutant experiments (c).

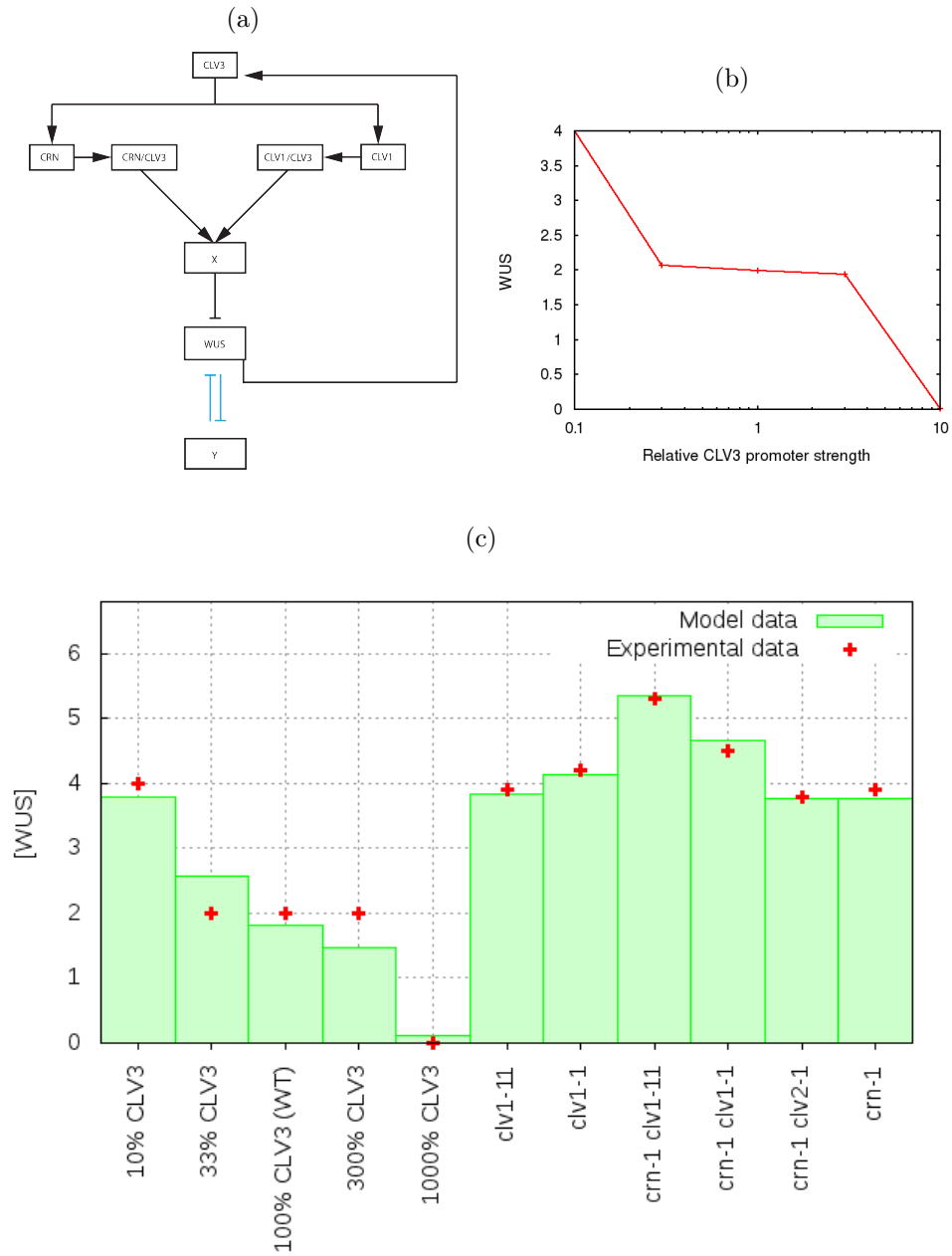Path 13 was modelled by replacing the base production of CLV1 with a hill-type repression by WUS, which has been indicated in large-scale experiments (Zhao et al., 2010). This model showed an excellent ability to account for the WUS buffering against *CLV3* perturbation (Figure 2.10b) but 50 optimizations failed to produce a parameter set that was able to explain the buffering while retaining the ability to explain the receptor mutant experiments (Figure 2.10c). It is worth noting that the base-line model is symmetrical in the receptor pathways and thus any results obtained from an altered CLV1 is directly applicable to the same scenario for CRN.
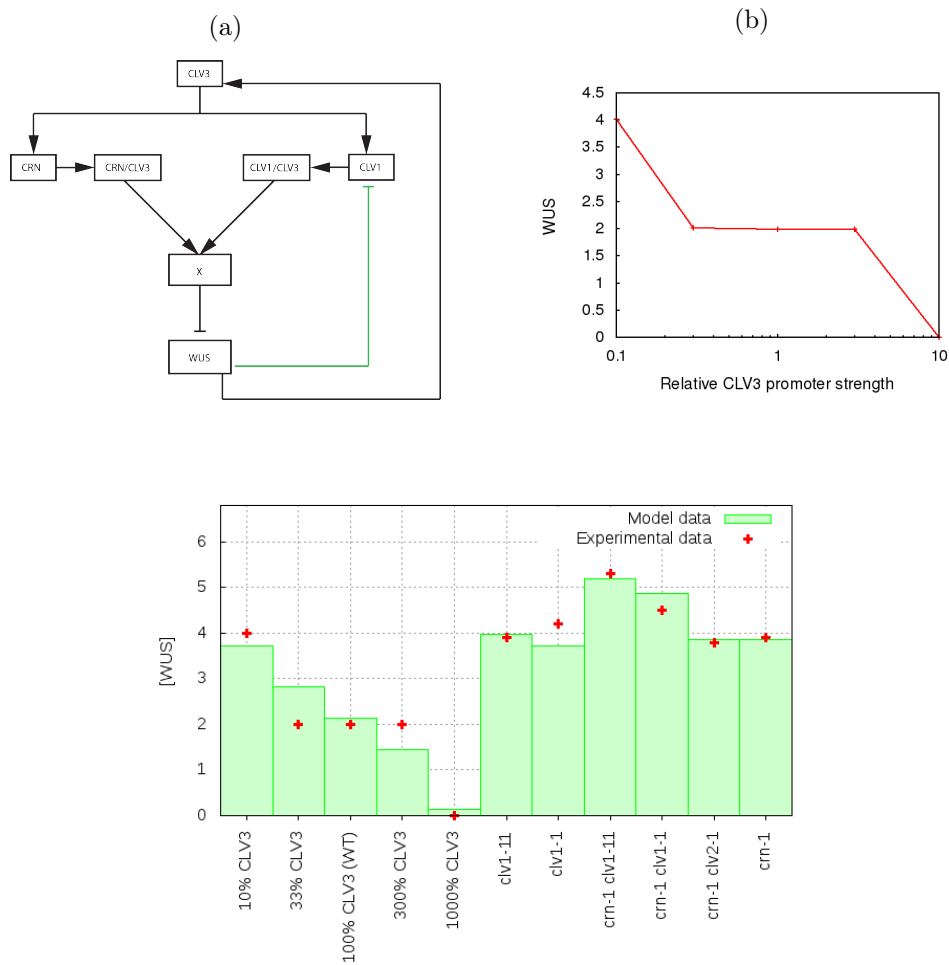

Figure 2.10: Model 13, where WUS acts as a repressor on CLV1 (a) were able to produce WUS buffering (b), but not at the same time as explaining the previously known mutant effects (c).
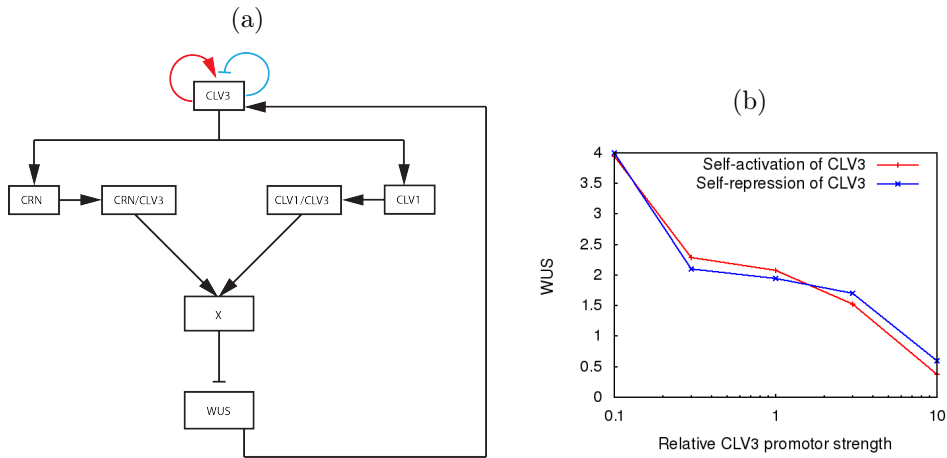
Figure 2.11: Models 3 and 4, which were self-interactions of CLV3 (a) did not produce the experimentally seen CLV3 perturbation data (b).

2.4   Alternative interactions in the CLV-WUS network

Both self-activation and self-repression of CLV3 was attempted but showed only a weak buffering-like dynamics when optimized solely against the WUS buffering (see figure 2.11). These model attempts were therefore not pursued further than the initial 25 optimizations.

Direct self-activation and self-repression of CLV1 were also modelled. Note once again that the receptor pathways is in this model mathematically identical before the optimizations, so all results from CLV1 interactions are also directly applicable to CRN. The results are represented in Figure 2.12 and they show that self activation of CLV1 (model 10) can produce some form of buffering even though the received energy value is relatively high and the WUS concentration does not reach zero as required. Self repression of CLV1 (model 11) however displays almost no tendencies to buffering at all.

Model 1 was created by replacing the linear activation of CLV3 by WUS with a Hill-type repression. The result showed no buffering capabilities at all and got a worse energy value than the unaltered model.

Model 5 was created by replacing the linear activation of CLV3 by WUS with a hill-type, non linear, activation. This produced fairly good results but was above the energy threshold for further investigation.

The results of models 1 and 5 are represented in figure 2.13.
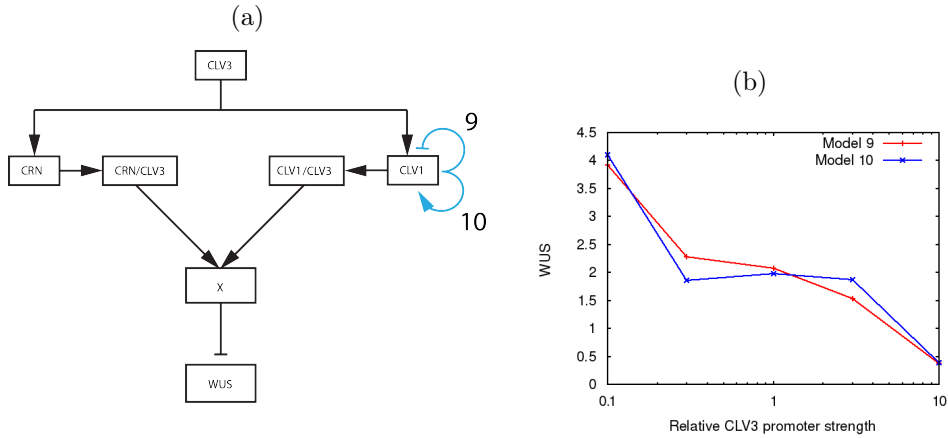
Figure 2.12: Direct self-interactions of CLV1 (a) did not manage to produce the WUS response to CLV3 promoter perturbations seen in experiments (b).
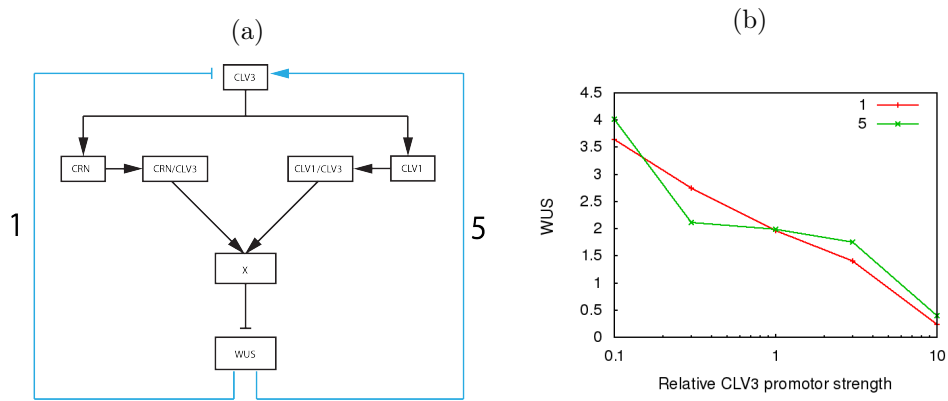
Figure 2.13: Model 1, which replaces the linear activation of CLV3 by WUS with a Hill-type repression (a) failed to produce buffering of WUS (b). Model 5, where the linear activation of CLV3 of WUS was instead replaced with a Hill-type activation (a) produced a form of buffering, even if it did not accurately reproduce the buffering data as required (b).

Chapter 3

Methods

3.1 Modelling strategy

The models were built non-spatially using mass action formalism together with a hill formalism for the modelling of transcriptions. All the models were relatively small alterations of the Sahlin et al. (2011) model which was used as a baseline model, defined by the following system of differential equations:

$$\frac{d[\text{CLV1}]}{dt} = t_1(s_1 - [\text{CLV1}]) - k_1[\text{CLV1}] \cdot [\text{CLV3}] \tag{3.1}$$
$$+ k_2[\text{CLV1/CLV3}]$$

$$\frac{d[\text{CRN}]}{dt} = t_2(s_2 - [\text{CRN}]) - k_4[\text{CRN}] \cdot [\text{CLV3}] \tag{3.2}$$
$$+ k_5[\text{CRN/CLV3}]$$

$$\frac{d[\text{CLV3}]}{dt} = t_3(s_3 - [\text{CLV3}]) + k_W[\text{WUS}] \tag{3.3}$$
$$- k_1[\text{CLV1}] \cdot [\text{CLV3}] + k_2[\text{CLV1/CLV3}]$$
$$- k_4[\text{CRN}] \cdot [\text{CLV3}] + k_5[\text{CRN/CLV3}]$$

$$\frac{d[\text{CLV1/CLV3}]}{dt} = k_1[\text{CLV1}] \cdot [\text{CLV3}] - k_2[\text{CLV1/CLV3}] \tag{3.4}$$
$$- t_1[\text{CLV1/CLV3}]$$

$$\frac{d[\text{CRN/CLV3}]}{dt} = k_4[\text{CRN}] \cdot [\text{CLV3}] - k_5[\text{CRN/CLV3}] \tag{3.5}$$
$$- t_2[\text{CRN/CLV3}]$$

$$\frac{d[\text{X}]}{dt} = t_4(s_4 - [\text{X}]) + k_3[\text{CLV1/CLV3}] + k_6[\text{CRN/CLV3}] \tag{3.6}$$

$$\frac{d[\text{WUS}]}{dt} = k_7\frac{K^n}{K^n + [\text{X}]^n} - d_W[\text{WUS}] \tag{3.7}$$

Where k_1 and k_4 is the reaction rates for the binding of CLV3 to the receptors and k_2 and k_5 the unbinding rate for the same. t_1, t_2, t_3 and t_4 is the degradation rate for the concentrations they effect while $t_1 s_1$, $t_2 s_2$, $t_3 s_3$ and $t_4 s_4$ is a constant, baseline, production rate for their respective molecule representation. k_3 and k_6 is the rates at which the bound states of the receptors produce X while k_7 provides the maximal production of WUS and the scale for the Hill function using X to repress the WUS production. K is a dissociation constant for the Hill function and n is the Hill exponent. k_W is the production rate constant for the linear activation of CLV3 by WUS and d_W is the degradation rate of WUS.

3.2 Mutants

All of the mutant representations require some form of alterations to the equations of section 3.1, especially to the parameters. But as the entire point of the optimization procedure is to produce a single parameter set that can account for all the network behavior the mutant representations were never allowed to alter the values of the parameters as displayed in the figure. Instead a number of dummy variables were added to the system of differential equations. These dummy variables were used either as binary switches for certain reactions or as discrete adjustments to the rate of the reactions.

The program was built up incrementally as more specific data was required to further the progress. The first step was to implement [CLV3Strength] which was used to represent the values of the *CLV3* promoter perturbations used in the experiments by Müller et al. (2006). 25 optimizations were performed for each of the attempted models (section 3.4). The models that recieved an energy value under 0.005 were investigated further.

After the initial evaluation of the proposed models binary dummy variables were added to allow the optimizer to find the overall best parameter set for 11 different systems representing the different mutants. The null mutants clv1-11, and crn-1 clv2-1 were modelled by activating their dummy variable (Table 3.1), which stopped the production of CLV1 or CRN respectively. The LOF mutants crn-1 and clv1-1 were treated differently from each other, activating the crn-1 dummy variable turned off the production of X from the bound CRN/CLV3 state, while activating the clv1-1 started an interference process that represents the receptors binding to each other and thereby losing their function.

During the build-up phase of the baseline model every major alteration was

$$\frac{d[\text{CLV1}]}{dt} = t_1(s_1[\text{clv1-11}] - [\text{CLV1}]) - k_1[\text{CLV1}][\text{CLV3}] \tag{3.8}$$
$$+ k_2[\text{CLV1/CLV3}] - k_m[\text{clv1-1}][\text{CLV1}][\text{CRN}]$$

$$\frac{d[\text{CRN}]}{dt} = t_2(s_2[\text{crn-1 clv2-1}] - [\text{CRN}]) - k_4[\text{CRN}][\text{CLV3}] \tag{3.9}$$
$$+ k_5[\text{CRN/CLV3}] - k_m[\text{clv1-1}][\text{CLV1}][\text{CRN}]$$

$$\frac{d[\text{CLV3}]}{dt} = t_3(s_3[\text{clv3Strength}] - [\text{CLV3}]) \tag{3.10}$$
$$+ k_W[\text{clv3Strength}][\text{WUS}] - k_1[\text{CLV1}][\text{CLV3}]$$
$$+ k_2[\text{CLV1/CLV3}] - k_4[\text{CRN}][\text{CLV3}] + k_5[\text{CRN/CLV3}]$$

$$\frac{d[\text{CLV1/CLV3}]}{dt} = k_1[\text{CLV1}][\text{CLV3}] - k_2[\text{CLV1/CLV3}] \tag{3.11}$$
$$- t_1[\text{CLV1/CLV3}]$$

$$\frac{d[\text{CRN/CLV3}]}{dt} = k_4[\text{CRN}][\text{CLV3}] - k_5[\text{CRN/CLV3}] \tag{3.12}$$
$$- t_2[\text{CRN/CLV3}]$$

$$\frac{d[\text{X}]}{dt} = t_4(s_4 - [\text{X}]) + k_3[\text{CLV1/CLV3}] \tag{3.13}$$
$$+ k_6[\text{crn-1}][\text{CRN/CLV3}]$$

$$\frac{d[\text{WUS}]}{dt} = k_7\frac{K^n}{K^n + [\text{X}]^n} - d_W[\text{WUS}] \tag{3.14}$$

Figure 3.1: The system of differential equations of the baseline model with the functions of all the mutant representations added. The parameters have interpretation as those of the same name in section 3.1. The only additional parameter is k_m which regulates the strength of the clv1-1 mutant.

Dummy variable	Activating value	Deactivating value
clv3Strength	0.1, 0.3, 3, 10	1
clv1-11	0	1
crn-1	0	1
clv1-1	1	0
crn-1 clv2-1	0	1

Table 3.1: Dummy variables used to emulate the mutants with the same name.

followed by an analysis in which the first step of a simulation with a given parameter set were compared with a pen and paper calculation of what the values and derivatives after this step should be. The equilibrium values were also compared with those that resulted from the program used by Sahlin et al. (2011) for their model to see that they matched when the clv3Strength was set to 1.

3.3 Model attempts

Tests were performed for 13 new interactions. They were implemented as follows:

Path 1 was modelled by replacing the $t_3 s_3[\text{clv3Strength}]$ term in eq. 3.10 of figure 3.1 with

$$s_3[\text{clv3Strength}] \frac{K_w^{n_w}}{K_w^{n_w} + [\text{WUS}]^{n_w}}$$

Path 2 was modelled by replacing the term

$$k_7 \frac{K^n}{K^n + [\text{X}]^n}$$

in eq 3.14 with:

$$k_7 \frac{K^n \cdot [\text{CLV3}]^{n_w}}{(K^n + [\text{X}]^n)(K_w^{n_w} + [\text{CLV3}]^{n_w})}$$

Path 3 was modelled by replacing the $t_3 s_3[\text{clv3Strength}]$ term in eq. 3.10 with:

$$s_3[\text{clv3Strength}] \frac{[\text{CLV3}]^{n_w}}{K_w^{n_w} + [\text{CLV3}]^{n_w}}$$

Path 4 was modelled by replacing the $t_3 s_3[\text{clv3Strength}]$ term in eq. 3.10 with:

$$s_3[\text{clv3Strength}] \frac{K_w^{n_w}}{K_w^{n_w} + [\text{CLV3}]^{n_w}}$$

Path 5 was modelled by replacing the $t_3 s_3[\text{clv3Strength}]$ term in eq. 3.10 with:

$$s_3[\text{clv3Strength}]\frac{[\text{WUS}]^{n_w}}{K_w^{n_w} + [\text{WUS}]^{n_w}}$$

Path 6 was modelled in two different ways: by *adding* or *multiplying* a hill activator in eq 3.14 and thus effectively replacing equation 3.14 by one of the following:

$$\frac{d[\text{WUS}]}{dt} = k_7 \frac{K^n \cdot [\text{WUS}]^{n_2}}{(K^n + [\text{X}]^n)(K_2^{n_2} + [\text{WUS}]^{n_2})} - d_W[\text{WUS}] \qquad (3.15)$$

$$\frac{d[\text{WUS}]}{dt} = k_7 \frac{K^n}{K^n + [\text{X}]^n} + k_w \frac{[\text{WUS}]^{n_2}}{K_2^{n_2} + [\text{WUS}]^{n_2}} - d_W[\text{WUS}] \qquad (3.16)$$

Both were used to test for wus buffering, but only the multiplied version (eq 3.15) were analysed further.

Path 7 was modelled by replacing the $k_7 \frac{K^n}{K^n + [\text{X}]^n}$ term in eq 3.14 by:

$$k_7 \frac{K^n \cdot K_2^{n_2}}{(K^n + [\text{X}]^n)(K_2^{n_2} + [\text{WUS}]^{n_2})}$$

Path 8 was modelled by replacing the $t_4 \cdot s_4$ term in eq 3.13 with:

$$s_4 \frac{K_w^{n_w}}{K_w^{n_w} + [\text{WUS}]^{n_w}}$$

Path 9 was modelled by replacing the $t_1 \cdot s_1[\text{clv1-11}]$ term in eq 3.8 with:

$$s_1[\text{clv1-11}]\frac{K_w^{n_w}}{K_w^{n_w} + [\text{CLV1}]^{n_w}}$$

Path 10 was modelled by replacing the $t_1 \cdot s_1[\text{clv1-11}]$ term in eq 3.8 with:

$$s_1[\text{clv1-11}]\frac{[\text{CLV1}]^{n_w}}{K_w^{n_w} + [\text{CLV1}]^{n_w}}$$

Path 11 was modelled by removing eq. 3.14 and instead adding to the figure 3.1 system of equations two additional equations:

$$\begin{cases} \frac{d[\text{WUS}]}{dt} & = & k_7 \frac{K^n \cdot [\text{Y}]^{n_2}}{(K^n + [\text{X}]^n)(K_2^{n_2} + [\text{Y}]^{n_2})} - d_W[\text{WUS}] \\\\ \frac{d[\text{Y}]}{dt} & = & k_y \frac{[\text{WUS}]^{n_y}}{K_y^{n_y} + [\text{WUS}]^{n_y}} - d_Y[\text{Y}] \end{cases} \qquad (3.17)$$

Path 12 was modelled by removing eq. 3.14 and instead adding to the figure 3.1 system of equations two additional equations:

$$
\begin{cases}
\frac{d[\text{WUS}]}{dt} &= k_7 \frac{K^n \cdot K_2^{n2}}{(K^n + [\text{X}]^n)(K_2^{n2} + [\text{Y}]^{n2})} - d_W[\text{WUS}] \\[2ex]
\frac{d[\text{Y}]}{dt} &= k_y \frac{K_y^{ny}}{K_y^{ny} + [\text{WUS}]^{ny}} - d_Y[\text{Y}]
\end{cases}
\tag{3.18}
$$

Path 13 was modelled by replacing the term $t_1 \cdot s_1[\text{clv1-11}]$ in eq 3.8 with:

$$
s_1[\text{clv1-11}] \frac{K_w^{n_w}}{K_w^{n_w} + [\text{WUS}]^{n_w}}
$$

3.4 Optimization

The optimization was done using a simulated annealing scheme (Kirkpatrick et al., 1983; Press et al., 2007) which followed a sequence of steps:

1. An initial set of parameters $p_{initial}$ were created by generating a random, real, number between 1 and 3 for the Hill parameters (all the parameters n, regardless of index) and between 0 and 1 for the rest of the parameters. This parameter set were then used for the simulations of step 2.

2. One simulation for each mutant was run. They ran for 400 time units using a fifth order Runge-Kutta solver with adaptive step size. The initial step size, and also the maximally allowed step size was 1.0 and the error allowance was 10^{-12}. After 400 time units the system would have equilibrated and the concentration of WUS was used to calculate an energy value according to:

$$
E = \sum_i ([\text{WUS}]_i - C_i)^2
\tag{3.19}
$$

   Where the sum is over all the different mutants and C_i the carpel numbers associated with the mutant, and is assumed to correlate with the total amount of WUS in a meristem.

3. A new parameter set p_{new} was proposed by choosing a random parameter from the old parameter set and, with equal chance, multiplying or dividing it by 1.01.

4. p_{new} was used in a repetition of step 2 and, with a probability of $P_{accept} = \min\left(1, e^{-\beta(E(p_{new}) - E(p_{old}))}\right)$ replaced the old parameter set.

5. Steps 1-4 were repeated for 1000 update attempts at each temperature $1/\beta$ which started at 1 and was multiplied by 0.9 until it reached 10^{-5}. The last parameter set that this method yielded was the one used as the result of the optimization.

Many simulations were run during the early stages of this research and equilibrium was reached before 100 time units in all observed cases. 400 time units was chosen for the optimization processes to ensure that the network always had time to stabilize, despite the changes that were made to the model.

Chapter 4

Discussion

It was shown that there are several different ways to modify the Sahlin et al. (2011) mass action, hill transcription model so that it produces the experimentally seen buffering dynamics. Although it would have been convenient to find that *one* model alteration produced excellent result and all the other conceivable alterations resulted definitively in an inability to produce the right dynamics it was not unexpected that this was not the case. A complete understanding of the stem cell regulatory network is not expected to be achieved in one single research project. The benefit of these particular results are numerous.

A primary result was the proof that by making a relatively small change to the computational model by Sahlin et al. (2011), and probably other models based on the negative feedback between CLV3 and WUS, an additional set of data that was previously unexplained can be explained. This shows that even if the simplistic model was falsified by the CLV3 promoter perturbations the major concept behind it is not.

It was also shown that addition of self-activation of WUS to the model, which is sufficient to explain the buffering, maintains the equipotency of the two receptor pathways (Figure 2.5a). This lends credence to the belief that the two pathways have an equal impact on the production of WUS.

Another result was to give pointers as to where further research is justified. A large amount of models were proposed and some worked excellently while other did not work at all. The self-activation of WUS in particular showed so much promise and versatility for both direct and indirect feedback that further modelling and experimental investigation would be justified. This is especially interesting in the light of the finding by Zhao et al. (2010) that WUS binds to proteins of the ARR family.

Self-activation of WUS was tested quite thoroughly. After seeing the suc-

cess of the direct version several indirect WUS activations were devised to see how well the results of direct activations transferred to indirect. The subsequent results show that although properties are not directly transferable some indirect activations does display similar dynamics to that of direct activation.

Thereby the success of WUS repressing X in the signaling pathway or activating an external factor Y indicate a likeliness of there being an unknown indirect self-activation of WUS either internally in the already known network or via an external network. The results also allow for some speculations about the indirect connection not being too indirect, as they somewhat indicate that a close self connection, with few intermediate steps works better than a connection of longer range.

It was unexpected that WUS repressing the repressor Y did not work when the activator counterpart and X repression did. With appropriately tuned parameters, which the optimizer should take care of, the dynamics of repressing the repressor Y could be quite similar to that of activating the activator Y. The dynamics when WUS repressed X is somewhat different to the dynamics of repressing Y since X with WUS as a repressor is doubly connected to WUS, but it was still unexpected that this would be the difference between success and failure. This observation may require some further investigation. The simplest investigation would be to run more optimizations in order to eliminate any statistical effects. But if this does not work then a detailed analysis of the modelling logic itself is called for.

An interesting point can be made from the parameters listed in the appendix where the value of k_m, the parameter regulating the effect that the clv1-1 mutant has, is consistently very high. In the model dynamics a very high value of this parameter will result in a very low concentration of one of the receptors CLV1 or CRN. This is a falsifiable statement and could be used to test the validity of the model.

The broad approach in testing many different model attempts led to an objective assessment of these attempts and to the finding of three truly viable model additions. Even though the positive results would not have benefitted from a more narrow approach with higher statistical accuracy the negative results would. The statistical inaccuracy means that the failed attempts can not from these results with certainty be rejected as candidates for the regulatory network. This is especially true for those models that were rejected after the first 25 optimizations. The precariousness of such a low number of optimizations is emphasized by the fact that the *multiplied* direct WUS self-activation model only got three successful parameter sets during these initial optimizations and yet that model turned out to be able to account for all the dynamics sought.

The activation of CLV3 by WUS in the baseline model is linear. While this reduces the number of parameters it is somewhat inconsistent with the type of modelling used for the suggested updates as WUS is a transcription factor. The suggested updates have all been non-linear and have been supposed to represent transcriptional reactions. When using this approach it would have made sense to change the baseline model in order to be consistent in the modelling techniques, but this was not done. The CLV3 activation was changed to a non-linear one in a few attempts, so the possibility of this reaction being the problem was not overlooked. But the reaction was left as a linear one for the rest of the attempts in order to keep the degree of freedom for the model down. The idea of doing so was to keep the number of false positives down, but it is never-the-less conceivable that it could have produced a false negative.

Despite this attempt to keep the models degree of freedom down the fact still remains that there is quite a large amount of free parameters. Many of these parameters are linearly dependent, so they do not each constitute a degree of freedom when optimizing the system. But there is still a danger of over-optimization when there are about twice as many parameters as there are data points against which to optimize. This is hard to avoid without extensive, expensive, experimentation, but the effects of limited data could in future research be mitigated by dividing the optimization procedure into validation pools, as done by Sahlin et al. (2011).

The number of parameters differed for the different model attempts, but the number of iterations of the optimizer did not. It could have made sense to keep the average number of updates per parameter constant and thus allowing them to cover the same range in each of the models, but this was not done. Instead the decrease in updates per parameter when increasing the number of parameters were kept as a form of penalty for the added degree of freedom of the system. With more added parameters, especially for the non-linear reactions that often were attempted, comes a stronger ability to fit *any* data, and this was penalized. It is possible to give an energy cost to the number of parameters (Lomax and Hahs-Vaughn, 2007), but since relatively few parameters were added it was not done in this initial investigation and was instead left for future research.

Hill formalism was used for modelling of transcription. Michaelis-Menten formalism would have had a lower degree of freedom, which is not a bad thing at all, but the Hill formalism was chosen. This was partly because of the dynamics the Hill exponent allows for, it provides a means of sharpening the sigmoidal curve that the reaction produces, which makes sense when looking for the type of buffering dynamics the CLV3 perturbations show. The other part of the reason for choosing a Hill formalism was how it allows for cooperative effects of the molecules simulated.

The modelling logic for multiple transcriptions to the same compound was mainly that of multiplying the hill equations with each other. A property this results in is that the reaction will halt if any activator has a concentration of zero, while a reaction with only repressors will have a base production that fairly quickly goes towards zero as the concentration of repressors goes to infinity. Another modelling logic was used in the *added* hill equations of eq. 3.16. But this logic also have some specific properties that may be unwanted; an infinite amount of repressors will not stop the production if there is any activators at all. It also has one extra parameter which may be considered a bad quality. The multiplied version was deemed the more representative of the options and was therefore used to a larger extent. A future project could be to investigate further the effects the choice of logic has on the network and correlate this to biological data or possibly even see if this may yield testable predictions as to how the small-scale reactions work.

Appendix

	1	2	3	4	5	StdDev
t_1	0.0461088	0.0704032	0.103227	0.0768508	0.0935173	0.019765
$t_1 \cdot s_1$	1.04223	1.13085	0.921652	0.415877	0.976577	0.250678
k_m	564.57	194.726	183.904	256.661	99.3173	160.402
t_2	0.0796362	0.108209	0.0781681	0.155493	0.0161939	0.045355
$t_2 \cdot s_2$	0.404389	0.481322	0.471885	0.449558	0.356501	0.0464576
$t_3 \cdot s_3$	5.75236	8.1904	6.89993	4.15578	0.0509163	2.81283
t_3	0.16782	0.184646	0.147577	0.0748002	0.298746	0.0724559
k_W	0.604878	0.282874	0.174243	0.19693	2.18794	0.764976
$t_4 \cdot s_4$	3.27925	4.1209	3.00346	0.741165	0.355905	1.48182
$1/s_4$	2.27058	0.800698	1.36145	2.69982	2.07323	0.676497
k_3	0.395188	0.202621	0.195896	0.0845212	0.261272	0.101311
k_6	1.72945	0.721043	0.294628	0.147171	0.123626	0.602577
k_7	0.571763	1.71173	1.71425	1.0756	0.524369	0.521649
K_2	0.448685	0.39192	0.527883	0.429439	0.435171	0.0447801
n_2	2.5351	2.86917	2.33533	2.61409	2.67107	0.174265
K	2.303	2.71496	1.31461	0.72071	6.11791	1.87911
n	2.77503	4.02222	3.63686	5.04691	2.50757	0.910728
d_w	0.106261	0.306067	0.276529	0.203801	0.097857	0.0852333
k_1	0.599896	1.30917	0.475919	0.780304	1.47441	0.394385
k_2	0.0582162	0.548655	0.204043	0.866578	0.157024	0.299523
k_4	1.06637	0.154505	0.715546	0.641257	1.73269	0.523563
k_5	0.459904	0.0408815	0.67191	0.467353	0.743573	0.2448
Energy	0.00157325	0.00331588	0.00864325	0.0101971	0.0104988	0.003690

Table 4.1: The five best parameter sets that was received from the optimisation of the direct WUS self-activation model.

Acronyms

SAM shoot apical meristem

> The region of a plant shoot that contains undifferentiated stem cells which can eventually, after differentiation give rise to new organs of the plant.

WUS WUSCHEL

> A transcription factor that is produced in the stem cells of the SAM.

CLV3 CLAVATA3

> A peptide produced in the stem cells of the SAM.

CLV1 CLAVATA1

> A receptor kinase found in the cell membrane of the cells in the OC and that binds to CLV3.

CRN CORYNE

> A protein that together with the protein CLV2 forms a receptor for CLV3 in the cell membrane of cells in the OC.

CZ Central Zone

> The centrally located region at the SAM apex in which the pluripotent stem cells can be found.

OC Organizing Center

> The zone beneath the CZ which excretes the transcription factor WUS and thereby plays a large part in the regulatory network of the SAM.

PZ Peripheral Zone

> The zone around the OC in which stem cells have begun their differentiation to form the tissue required for the growth of the plant.

LOF Loss-of-function

> A description of the effect of a mutant. The mutated gene may produce a protein which still functions, but not as efficiently as the wild type.

WT wild-type

> The normal, non-mutated version of a plant.

Bibliography

R Sablowski. The dynamic plant stem cell niches. *Curr Opin Plant Biol*, 10 (6):639–44, 2007.

A Bleckmann and R Simon. Interdomain signaling in stem cell maintenance of plant shoot meristems. *Mol Cells*, 27(6):615–20, 2009.

Heiko Schoof, Michael Lenhard, Achim Haecker, Klaus F.X Mayer, Gerd Jürgens, and Thomas Laux. The stem cell population of arabidopsis shoot meristems is maintained by a regulatory loop between the clavata and wuschel genes. *Cell*, 100(6):635 – 644, 2000.

Elliot M Meyerowitz. Genetic control of cell division patterns in developing plants. *Cell*, 88(3):299 – 308, 1997.

Jennifer C. Fletcher, Ulrike Brand, Mark P. Running, Rüdiger Simon, and Elliot M. Meyerowitz. Signaling of cell fate decisions by clavata3 in arabidopsis shoot meristems. *Science*, 283(5409):1911–1914, 1999.

Klaus F.X Mayer, Heiko Schoof, Achim Haecker, Michael Lenhard, Gerd Jürgens, and Thomas Laux. Role of wuschel in regulating stem cell fate in the arabidopsis shoot meristem. *Cell*, 95(6):805 – 815, 1998.

Steven E Clark, Robert W Williams, Elliot M Meyerowitz, et al. The clavata1 gene encodes a putative receptor kinase that controls shoot and floral meristem size in arabidopsis. *Cell*, 89(4):575, 1997.

R Muller, A Bleckmann, and R Simon. The receptor kinase coryne of arabidopsis transmits the stem cell-limiting signal clavata3 independently of clavata1. *Plant Cell*, 20(4):934–46, 2008.

Ram Kishor Yadav, Mariano Perales, Jeremy Gruel, Thomas Girke, Henrik Jonsson, and G. Venugopala Reddy. WUSCHEL protein movement mediates stem cell homeostasis in the Arabidopsis shoot apex. *GENES & DEVELOPMENT*, 25(19):2025–2030, 2011.

Patrik Sahlin, Pontus Melke, and Henrik Jonsson. Models of sequestration and receptor cross-talk for explaining multiple mutants in plant stem cell regulation. *BMC Systems Biology*, 5(1):2, 2011.

Ram Kishor Yadav, Montreh Tavakkoli, and G Venugopala Reddy. Wuschel mediates stem cell homeostasis by regulating stem cell number and patterns of cell division and differentiation of stem cell progenitors. *Development*, 137(21):3581–3589, 2010.

T Laux, KFX Mayer, J Berger, and G Jurgens. The WUSCHEL gene is required for shoot and floral meristem integrity in Arabidopsis. *Development*, 122(1):87–96, 1996.

GV Reddy and EM Meyerowitz. Stem-cell homeostasis and growth dynamics can be uncoupled in the Arabidopsis shoot apex. *SCIENCE*, 310(5748): 663–667, 2005.

Tim Hohm, Eckart Zitzler, and Rüdiger Simon. A dynamic model for stem cell homeostasis and patterning in arabidopsis meristems. *PLoS ONE*, 5 (2), 02 2010.

Hironori Fujita, Koichi Toyokura, Kiyotaka Okada, and Masayoshi Kawaguchi. Reaction-diffusion pattern in shoot apical meristem of plants. *PLoS ONE*, 6(3), 03 2011.

Ram Kishor Yadav, Mariano Perales, Jérémy Gruel, Carolyn Ohno, Marcus Heisler, Thomas Girke, Henrik Jönsson, and G Venugopala Reddy. Plant stem cell maintenance involves direct transcriptional repression of differentiation program. *Molecular systems biology*, 9(1), 2013.

Ralf Müller, Lorenzo Borghi, Dorota Kwiatkowska, Patrick Laufs, and Rüdiger Simon. Dynamic and compensatory responses of arabidopsis shoot and floral meristems to clv3 signaling. *The Plant Cell Online*, 18(5):1188–1198, 2006.

Henrik Jönsson. Systems biology, lecture notes, 2012.

Zhong Zhao, Stig U Andersen, Karin Ljung, Karel Dolezal, Andrej Miotk, Sebastian J Schultheiss, and Jan U Lohmann. Hormonal control of the shoot stem-cell niche. *Nature*, 465(7301):1089–1092, 2010.

Scott Kirkpatrick, D. Gelatt Jr., and Mario P Vecchi. Optimization by simulated annealing. *science*, 220(4598):671–680, 1983.

William H Press, Saul A Teukolsky, William T Vetterling, and Brian P Flannery. *Numerical recipes 3rd edition: The art of scientific computing.* Cambridge university press, 2007.

Richard G Lomax and Debbie L Hahs-Vaughn. *Statistical concepts: a second course.* Lawrence Erlbaum Associates Mahwah, 2007.